Glacial-interglacial circulation changes inferred from $^{231}Pa/^{230}Th$ sedimentary record in the North Atlantic region

J.-M. Gherardi,[1] L. Labeyrie,[2] S. Nave,[3] R. Francois,[4] J. F. McManus,[5] and E. Cortijo[2]

Received 6 October 2008; revised 19 November 2008; accepted 8 January 2009; published 2 May 2009.

[1] Studies from the subtropical western and eastern Atlantic Ocean, using the $^{231}Pa/^{230}Th$ ratio as a kinematic proxy for deep water circulation, provided compelling evidence for a strong link between climate and the rate of meridional overturning circulation (MOC) over the last deglaciation. In this study, we present a compilation of existing and new sedimentary $^{231}Pa/^{230}Th$ records from North Atlantic cores between 1710 and 4550 m water depth. Comparing sedimentary $^{231}Pa/^{230}Th$ from different depths provides new insights into the evolution of the geometry and rate of deep water formation in the North Atlantic during the last 20,000 years. The $^{231}Pa/^{230}Th$ ratio measured in upper Holocene sediments indicates slow water renewal above ~2500 m and rapid flushing below, consistent with our understanding of modern circulation. In contrast, during the Last Glacial Maximum (LGM), Glacial North Atlantic Intermediate Water (GNAIW) drove a rapid overturning circulation to a depth of at least ~3000 m depth. Below ~4000 m, water renewal was much slower than today. At the onset of Heinrich event 1, transport by the overturning circulation declined at all depths. GNAIW shoaled above 3000 m and significantly weakened but did not totally shut down. During the Bølling-Allerød (BA) that followed, water renewal rates further decreased above 2000 m but increased below. Our results suggest for the first time that ocean circulation during that period was quite distinct from the modern circulation mode, with a comparatively higher renewal rate above 3000 m and a lower renewal rate below in a pattern similar to the LGM but less accentuated. MOC during the Younger Dryas appears very similar to BA down to 2000 m and slightly slower below.

Citation: Gherardi, J.-M., L. Labeyrie, S. Nave, R. Francois, J. F. McManus, and E. Cortijo (2009), Glacial-interglacial circulation changes inferred from $^{231}Pa/^{230}Th$ sedimentary record in the North Atlantic region, *Paleoceanography*, *24*, PA2204, doi:10.1029/2008PA001696.

1. Introduction

[2] Understanding the links between changes in climate and ocean's meridional overturning circulation is a major challenge in paleoclimatology [*Gregory et al.*, 2005]. Variations in past ocean circulation have been inferred from records of the deep water chemical composition derived from sedimentary nutrient proxies such as $\delta^{13}C$ [*Curry and Oppo*, 2005; *Duplessy et al.*, 1988] or Cd/Ca [*Boyle and Keigwin*, 1987] in benthic foraminifera, but these measurements do not constrain the rate of overturning [*Boyle and Keigwin*, 1987; *Legrand and Wunsch*, 1995]. Furthermore, they can be overwritten by secondary effects such as biological productivity, regional air-sea exchange, changes in bottom water calcite saturation [*Lynch-Stieglitz et al.*, 1995; *Mackensen et al.*, 1993; *Marchitto et al.*, 2000], or water masses properties changes [*Lynch-Stieglitz et al.*, 2007] [*Gebbie and Huybers*, 2006]. Nd isotopes ratios (ε_{Nd}) of authigenic ferromanganese oxides, a water mass tracer which is independent of nutrient cycling, seems promising [*Piotrowski et al.*, 2004] but its interpretation remains controversial because of potential isotopic exchange along the water trajectories, or changes in the ε_{Nd} signature at the source [*Tachikawa et al.*, 2003]. In response to those problems, several kinematic tracers of ocean overturning are being developed. Paired planktonic-benthic ^{14}C age differences or ^{14}C ages of ^{230}Th-dated deep sea corals can potentially provides estimates of deep water renewal rates [*Keigwin and Schlegel*, 2002; *Robinson et al.*, 2005]. Complications arise however from the need to take into account possible changes in reservoir ages and the variability of $\Delta^{14}C$ of the atmosphere. Density gradient in the main thermocline and below has also been obtained from oxygen isotope measurements ($\delta^{18}O$) on benthic foraminifera to estimate past meridional transport from geostrophic calculations [*Came et al.*, 2008; *Lynch-Stieglitz et al.*, 1999]. The main difficulty here is the requirement that current velocity must be known at one level taken as reference, which is very difficult to obtain for past circulation [*Wunsch*, 2003]. Finally, excess sedimentary

[1]Bjerknes Center for Climate Research, University of Bergen, Bergen, Norway.
[2]Laboratoire des Sciences du Climat et de l'Environnement, CNRS, Gif-sur-Yvette, France.
[3]Departamento de Geologia Marinha, Instituto Nacional de Engenharia, Tecnologia e Inovação, Amadora, Portugal.
[4]Department of Earth and Ocean Sciences, University of British Columbia, Vancouver, British Columbia, Canada.
[5]Department of Geology and Geophysics, Woods Hole Oceanographic Institution, Woods Hole, Massachusetts, USA.

0883-8305/09/2008PA001696$12.00

$^{231}Pa/^{230}Th$ (activity ratios of ^{231}Pa and ^{230}Th not supported by U present in the sediment mineral lattices, decay corrected to the time of deposition; Pa/Th hereafter) has also been proposed as a dynamic proxy to record changes in Atlantic meridional overturning circulation (AMOC) [*Yu et al.*, 1996; *McManus et al.*, 2004]. However, Pa/Th recorded in the sediments can be affected by changes in particle flux and composition [*Chase et al.*, 2002], which can obscure its interpretation in terms of changes in circulation. In addition, the extent to which sediment Pa/Th records water renewal at depth shallower than the coring site has also been questioned [*Thomas et al.*, 2006] in an Indian ocean site study. This paper aims at further investigating the potential of this tool as a paleocirculation proxy.

[3] Recently, *Gherardi et al.* [2005] compared the results obtained from the West Atlantic core OCE326-GGC5 (33°42′N, 57°35′W, 4550 m, named GGC5 hereafter) [*McManus et al.*, 2004] with a record from the Iberian Margin (SU81-18; 37°46′N, 10°11′W, 3135 m). Notwithstanding the different depths and sedimentary settings from which the two Pa/Th profiles were obtained, they showed strong similarities, lending support to the interpretation of Pa/Th as mostly reflecting changes in the rate of the Atlantic meridional overturning. Both records suggest a significant decrease of the rate of the Atlantic MOC during Heinrich 1 (H1) and Younger Dryas.

[4] A modeling study [*Siddall et al.*, 2007] has recently pointed out that the spatial distribution of Pa/Th in the North Atlantic could give a convincing fingerprint of changes in the strength of the Atlantic Meridional Oceanic Circulation (AMOC). We are here comparing the deglacial Pa/Th record from six North Atlantic cores (three already published and three new data sets) spanning the depth interval from 1700 m to 4550 m. The cores locations span a wide range of sedimentary environments including large-scale hemipelagic sedimentation, distal open ocean pelagic sedimentation, and highly variable pulses of deposition of ice-rafted detritus (IRD). We focus our discussion mostly on the contrasting evolution of sediment Pa/Th in the North Atlantic as a function of water depth, which provides new insight into changes in the strength and geometry of the AMOC during the last deglaciation and further confirms the potential of sediment Pa/Th as a dynamic tracer of ocean circulation while highlighting some of the pitfalls of the method.

2. Pa/Th Ratio as a Paleocirculation Proxy

[5] Sediment Pa/Th records past changes in the rate of the MOC as a result of the difference in particle reactivity between ^{231}Pa and ^{230}Th in the water column [*Yu et al.*, 1996]. Both nuclides (^{231}Pa half-life $t_{1/2}$ = 32.5 ka and ^{230}Th $t_{1/2}$ = 75.2 ka) are produced at a constant initial Pa/Th activity ratio of 0.093 from the decay of dissolved uranium in the ocean [*Turekian and Chan*, 1971]. ^{230}Th is the most particle reactive, with very short residence times in the water column limiting redistribution by horizontal transport. In contrast, the residence time of ^{231}Pa (100–200 years) [*Nozaki and Nakanishi*, 1985] is similar to the residence time of deep water in the Atlantic [*Broecker*, 1979]. Consequently, the modern Atlantic overturning circulation exports approximately half the ^{231}Pa produced in deep water during its transit across the Atlantic and Pa/Th in Atlantic sediment is only half the production rate ratio [*Yu et al.*, 1996]. Past decreases in the rate of the Atlantic overturning would translate into higher Atlantic sediment Pa/Th, which would reach the production rate ratio for a total shutdown. The potential of sediment Pa/Th as a tracer of Atlantic ocean overturning rate has recently been supported by modeling experiments conducted with a zonally averaged Ocean Coupled Model (OCM) and a 3D model of intermediate complexity [*Marchal et al.*, 2000; *Siddall et al.*, 2005, 2007].

[6] A complication with this approach is that changes in scavenging intensity, controlled by particle flux and composition, can also influence sedimentary Pa/Th [*Chase et al.*, 2003; *Geibert and Usbeck*, 2004; *Scholten et al.*, 2008; *Siddall et al.*, 2007; *Walter et al.*, 1997]. Higher particle flux could increase sediment Pa/Th independently of circulation [*Anderson et al.*, 1983a]. Likewise, biogenic silica has a strong affinity for ^{231}Pa [*Chase et al.*, 2002] and higher opal concentration in settling particles could also increase sediment Pa/Th by reducing considerably the fractionation between both radionuclides. However, because the North Atlantic (1) has a vigorous overturning, (2) is close to the site of NADW formation, and (3) has low ^{231}Pa and ^{230}Th in its surface waters, circulation is the predominant factor controlling sedimentary Pa/Th. Nonetheless, it is essential to consider possible biases resulting from changes in particle flux and composition before interpreting sedimentary Pa/Th profiles in terms of circulation changes. This is achieved by measuring biogenic silica [*Nave et al.*, 2007] and evaluating past changes in particle flux by ^{230}Th normalization. The latter is based on the fact that, as a result of its very short residence time in the water column, the flux of ^{230}Th to the seafloor is nearly everywhere approximately equal to its well-constrained production rate [*Anderson et al.*, 1983b; *Bacon*, 1984; *Henderson et al.*, 1999; *Hoffmann and McManus*, 2007; *McManus et al.*, 1998]. Normalizing particle flux to the known production rate of ^{230}Th in the water column thus provides a mean of estimating the preserved rain rates of particles and their constituents to the seafloor [*Francois et al.*, 2004; *Yu et al.*, 2001]. Here, we have used this approach to estimate past changes in total mass, and opal fluxes.

3. Method and Material

3.1. Analytical Procedures

[7] Uranium, thorium and protactinium were measured by isotope dilution on a Finnigan MAT Element 2, single collector, sector field, inductively coupled plasma mass spectrometer [*Choi et al.*, 2001] (adapted to sediment measurements) The samples (typically 0.3–0.4 g) were ground with mortar and pestle, then spiked with ^{233}Pa [*Anderson and Fleer*, 1982] and ^{229}Th before total dissolution in HNO_3, HF and $HClO_4$. An aliquot of the resulting solution was removed, spiked with ^{236}U and another ^{229}Th, and analyzed for ^{238}U and ^{232}Th. The remaining solution was used for ^{231}Pa and ^{230}Th separation by ion exchange chromatography.

Table 1. The ^{14}C AMS Data Points and Calendar Ages for Core NA87-22 and Chronostratigraphic Tight Points for SU90-44[a]

NA87-22			SU90-44	
Depth (cm)	^{14}C Age (ka)	Calendar Age (ka)	Depth (cm)	Calendar Age (ka)
0	0.94	0.54	10	2.17
20	1.28	0.83	44	11.43
50	2.57	2.04	46	13.29
80	3.23	3.12	49	13.64
95	3.52	3.65	50	13.87
150	6.29	6.61	61	14.84
180	7.63	7.94	67	16.48
200	8.28	8.74	110	21.48
225	8.79	9.39		
250	10.01	10.40		
270	10.87	11.36		
285	11.32	12.41		
305	11.69	13.50		
315	12.32	14.02		
325	12.92	14.17		
345	14.58	14.80		
355	15.66	15.97		
370	15.80	16.73		
380	16.70	17.79		
400	17.59	19.33		
420	18.11	20.36		
440	19.31	21.77		

[a]The ^{14}C AMS data points are used as a stratigraphic reference.

[8] Excess activities were obtained by correcting for the supported detrital portion of the ^{230}Th and ^{231}Pa calculated using a lithogenic ^{238}U/^{232}Th activity ratio appropriate to the North Atlantic ocean (0.6 ± 0.1 [*Henderson and Anderson*, 2003; *McManus et al.*, 2004; *Walter et al.*, 1997]). Each estimate of excess ^{231}Pa and ^{230}Th was corrected for radioactive decay and ingrowth from authigenic uranium since the time of deposition determined from the ^{14}C-based age model (Tables 1, 2, and 3). All the new ^{231}Pa, ^{230}Th and Pa/Th ratios, as well as ^{230}Th-normalized fluxes, are presented in Data Set S1 in the auxiliary material.[1]

[9] Diatoms are quantified following the counting procedure of *Schrader and Schuette* [1968]. Diatoms counts were converted to valves/g of sediment. Preserved fluxes were then evaluated by ^{230}Th normalization [*Nave et al.*, 2007] (see also Text S1 in the auxiliary material for more details).

[10] The opal fluxes have been calculated only within the LGM-H1 transition for the most northern cores SU90-44 and MD95-2027 [*Nave et al.*, 2007], when changes in opal productivity are likely to occur [*Abrantes*, 2000]. The opal fluxes have been reconstructed for the entire Holocene and most of the deglaciation for the mid-Atlantic ridge core MD95-2037.

3.2. Core Settings and Stratigraphies

[11] In this description of the new sites, as for the rest of the paper, the cores will be discussed starting from the deepest to the shallowest.

[12] Sites OCE326-GGC5 on the Bermuda Rise, SU81-18 on the Iberian Margin and DAPC2 in the northern Rockall Trough (Figure 1), have been previously described in detail [*McManus et al.*, 2004; *Gherardi et al.*, 2005; *Hall et al.*, 2006]. All have robust age models constraining the last deglaciation with 16, 22 and 14 ^{14}C AMS ages respectively.

[13] SU90-44 (50°01′N, 17°06′W, 4279 m) is located in the northeastern Atlantic basin, near the top of a small abyssal hill, southeast of the Rockall plateau. Surface waters at the site lie within the North Atlantic Current (NAC) and at depth it is bathed by the Wyville-Thomson Ridge Overflow (WTRO), one of the water masses constituting NADW. The core is also at the northern boundary of the modern influence of Antarctic Bottom Water (AABW). The age model of core SU90-44 was established using correlations with the previously dated core NA87-22 (55°29 N, 14°41W, 2161 m) located further north (Figure 1) [*Waelbroeck et al.*, 2001, 2006]. The strongest constraints of the age model are concentrated around H1 through IRD and planktonic foraminifera oxygen isotope correlation (Figure 2c). Because of its relatively low sedimentation rate $\leq$ 5 cm/1000 years, the age model of this core remains poorly constrained over the latter part of the deglaciation (Table 1). The focus was put on the LGM-H1 transition, so that high sampling resolution (every centimeter, representing approximately 200 year resolution) was made between 58 and 62 cm, whereas the deglaciation was not studied at such high resolution (2–5 cm sample spacing representing approximately 500–1000 year resolution).

[14] MD95-2027 (41°44′N, 47°44′W, 4112 m) is located at the base of the Newfoundland margin, (Figure 1) near the boundary between the warm North Atlantic surface Current (NAC) and the polar Labrador Current (LC). It is a replicate of the studied and dated core CH69-K09 (41°45′N, 47°21′W, 4100 m) [*Cortijo et al.*, 1997; *Labeyrie et al.*, 1999]. As OCE326-GGC5, the site is swept by the lower North Atlantic deep Water (NADW) contour current and should record a similar circulation signal. This core was studied only within the LGM and H1 intervals, at high resolution. MD95-2027 has a high hemipelagic sedimenta-

Table 2. The ^{14}C AMS Data Points and Calendar Ages for Core CH69-K09 and Chronostratigraphic Tight Points for MD95-2027[a]

CH69-K09			MD95-2027	
Depth (cm)	^{14}C Age (ka)	Calendar Age (ka)	Depth (cm)	Calendar Age (ka)
0	1.15	0.55	239	10.56
20	2.24	2.03	280	11.43
33	3.13	3.08	388	15.36
52	4.77	4.86	406	15.87
85	6.66	7.02	417	16.69
130	8.84	9.25	428	17.70
175	9.69	10.27	439	18.84
215	11.14	11.97		
230	12.33	13.49		
280	13.63	14.60		
300	14.97	16.22		
320	18.02	19.13		

[a]The ^{14}C AMS data points are used as a stratigraphic reference.

[1]Auxiliary material data set is available at ftp://ftp.agu.org/apend/pa/2008pa001696. Other auxiliary material files are in the HTML.

Table 3. The ^{14}C AMS Data Points and Calendar Ages for MD95-2037

Depth (cm)	^{14}C Age (ka)	Calendar Age (ka)
1	3.47	3.34
40	5.51	5.88
100	9.59	10.43
151	10.52	11.66
190	10.93	12.52
260	11.76	13.22
330	13.69	15.77
390	16.64	19.33
451	21.42	25.21

tion rate, that ranges 10–30 cm/ka, and the age model was established using IRD peaks and planktonic foraminifera oxygen isotopes to correlate with and transfer the chronology of the well-dated nearby core CH69-K09 (Figure 2b) [*Waelbroeck et al.*, 2001]. The resulting resolution of the Pa/Th record is better than 300 years (Figure 2b and Table 2).

[15] These two Northern sites (MD95-2027 and SU90-44) (Figure 1) are located within polar waters during the glacial period and early deglaciation. *Waelbroeck et al.* [2001] have shown that in these areas surface water ^{14}C reservoir ages may exceed 1000 years during periods of extensive sea ice cover and strong near surface halocline. Another limitation for their age models stems from the highly varying sedimentation rate in these cores, both located within the zone of high IRD input during Heinrich events [*Grousset et al.*, 1993], and much lower sedimentation rate in between. This is particularly true for core MD95-2027, located near the area of maximum input flux of IRD. Age models are constrained by regional correlation of the temporal changes in sedimentary and foraminiferal proxies.

[16] Core MD95-2037 (37°05′N, 32°01′W, 2150 m) was taken on the eastern slope of the Mid-Atlantic Ridge, in the vicinity of the Lucky Strike hydrothermal field. This area is presently dominated by relatively warm conditions associated with the subtropical North Atlantic gyre. Estimates of

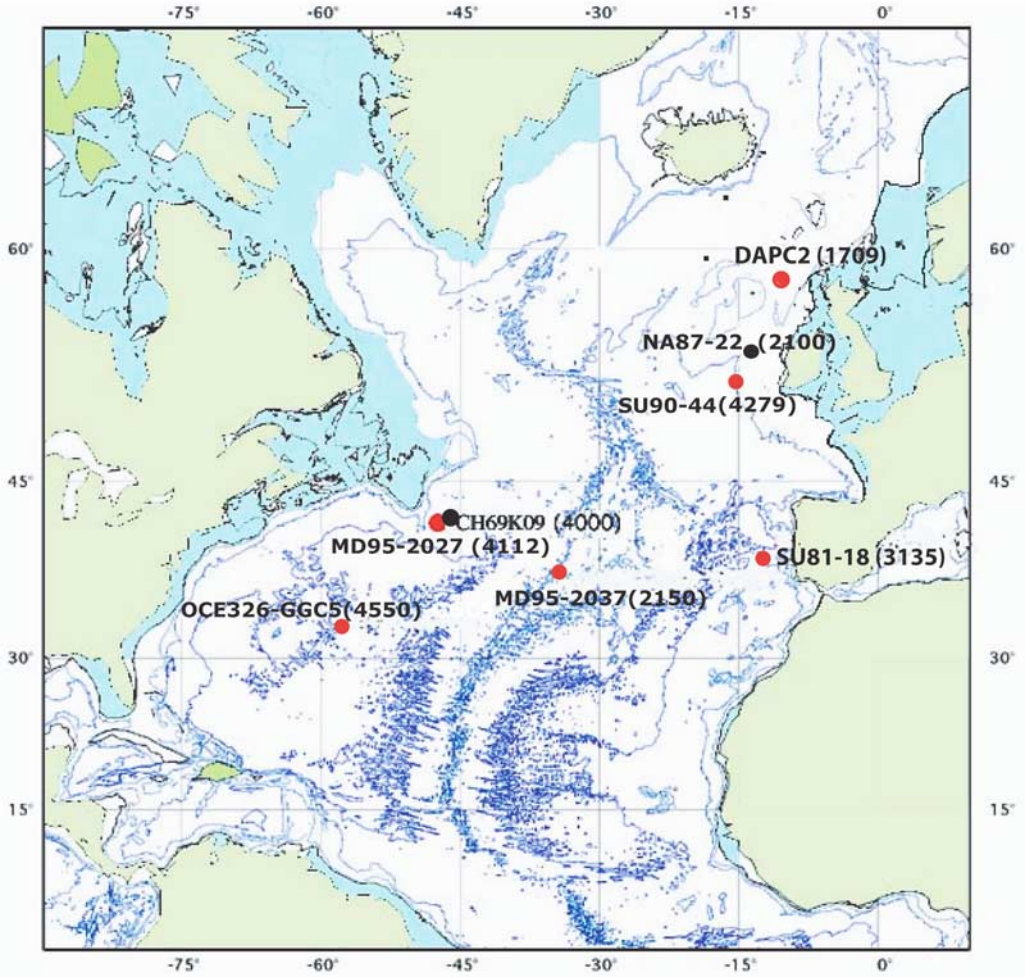

Figure 1. Map of the North Atlantic showing studied site locations (red dots) and sites used for stratigraphic correlations (black dots). OCE326-GGC5: 33°42′N, 57°35′W; depth 4550 m. MD95-2027: 41°44′N, 47°44′W; depth 4112 m and CH69-K09: 41°45′N, 47°21′W; depth 4100 m. SU90-44: 50°01′N, 17°06′W; depth 4279 m and NA87-22: 55°29′N, 14°41′W; depth 2161 m. SU81-18: 37°46′N, 10°11′W; depth 3135 m. MD95-2037: 37°05′N, 32°01′W; depth 2150 m. DAPC2: 58°58′N, 09°36′W; depth 1709 m.

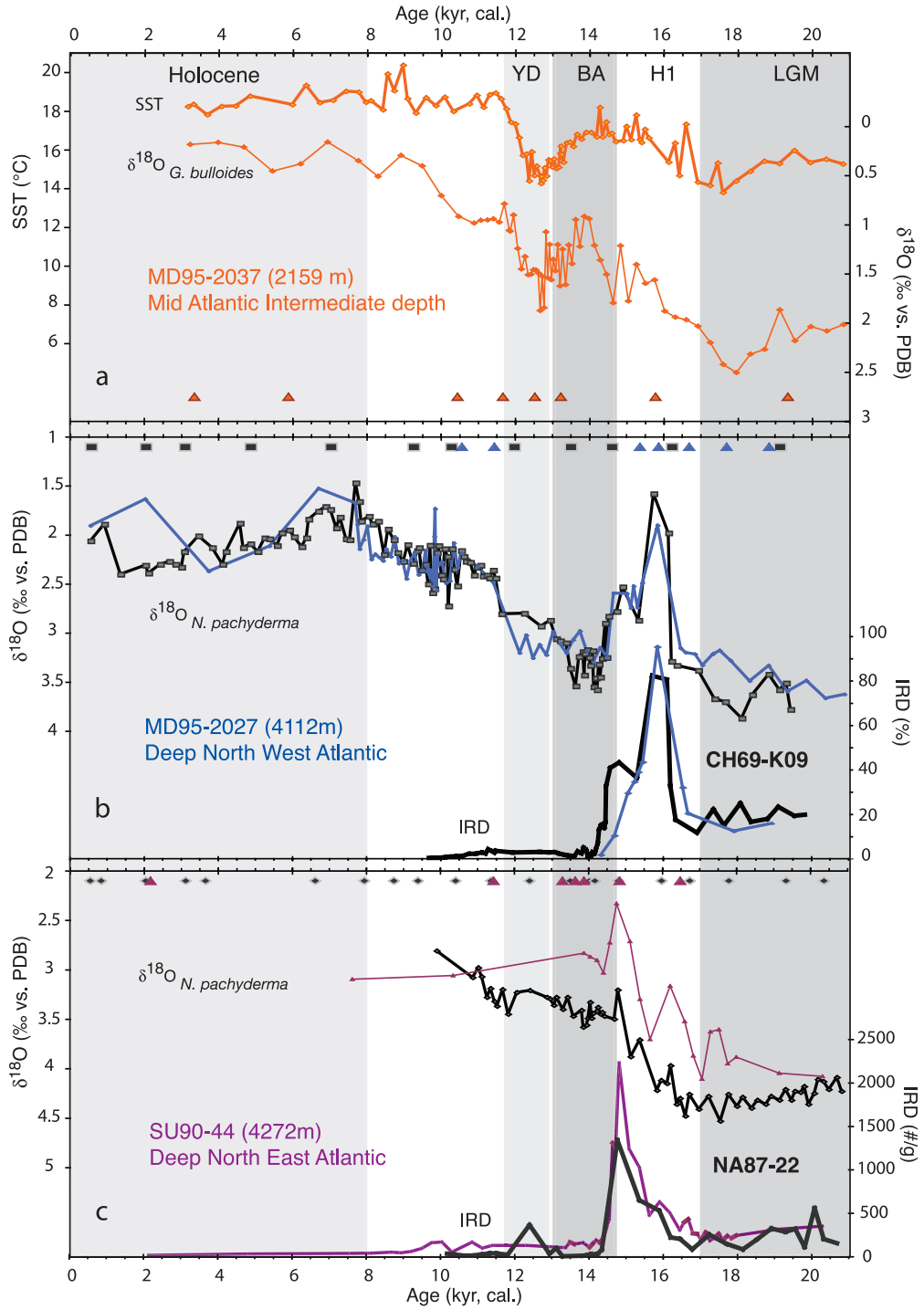

Figure 2. Core stratigraphy; cores have been ordered by depth. (a) SST [*Calvo et al.*, 2001] and *Globigerina bulloides* oxygen isotopes data (top and bottom curves, respectively) from sediment core MD95-2037. The ^{14}C AMS dating points are shown by the orange triangles. (b) IRD and *Neogloboquadrina pachyderma* (left) oxygen isotope data (bottom and top curves, respectively) from sediment core CH69-K09 (black curve) used as a stratigraphic reference [*Waelbroeck et al.*, 2001] compared with MD95-2027 oxygen isotope data (blue curve). Squares show the ^{14}C AMS dating points of CH69-K09, and blue triangles show the tie points used for the MD95-2027 age model. (c) IRD and *Neogloboquadrina pachyderma* (left) oxygen isotope data (bottom and top curves, respectively) from sediment core SU90-44 (purple curves) compared with NA87-22 (black curves) for stratigraphic correlations. NA87-22 ^{14}C AMS dating points are shown by the dark gray diamonds [*Waelbroeck et al.*, 2001], and the tie points used for SU90-44 age model are shown by the purple triangles.

Table 4. Pa/Th Means of the Studied Core for Selected Time Slices[a]

Core	Depth (m)	Pa/Th	2σ Error
	Holocene (0–8 ka)		
GGC5	4555	0.055	0.002
SU90-44	4279	0.052	0.004
SU81-18	3135	0.064	0.004
MD95-2037	2100	0.093	0.012
DAPC2	1709	0.094	0.002
	YD (11.6–12.8 ka)		
GGC5	4555	0.073	0.002
SU90-44	4279		
SU81-18	3135	0.075	0.003
MD95-2037	2100	0.053	0.001
DAPC2	1709	0.081	0.004
	BA (13–14.5 ka)		
GGC5	4555	0.070	0.003
SU90-44	4279	0.072	0.002
SU81-18	3135	0.068	0.004
MD95-2037	2100	0.053	0.002
DAPC2	1709	0.078	0.002
MD95-2027	4100	0.085	0.006
	H1 (15–17 ka)		
GGC5	4555	0.083	0.004
SU90-44	4279	0.088	0.004
SU81-18	3135	0.074	0.004
MD95-2037	2100	0.059	0.002
DAPC2	1709	0.065	0.003
MD95-2027	4100	0.083	0.008
	LGM (18–21 ka)		
GGC5	4555	0.067	0.003
SU90-44	4279	0.079	0.004
SU81-18	3135	0.049	0.004
MD95-2037	2100	0.041	0.002
DAPC2	1709	0.053	0.002
MD95-2027	4100	0.080	0.003

[a]YD, Younger Dryas; BA, Bølling-Allerød. Periods of transition were not included in the calculation of these means (H1 Pa/Th value of core SU81-18 was calculated between 16.3 and 15 ka, and mean upper Holocene Pa/Th value for core MD95-2037 includes only data from 7 to 3 ka) partly to avoid chronological uncertainties.

Sea Surface Temperature (SST) over the last climatic cycle [*Calvo et al.*, 2001] show that this location remained south of the polar front (Figure 2a, top curve) [*CLIMAP Project Members*, 1984]. At present, MD95-2037 is bathed at depth by the southward flow of the Upper North Atlantic Deep Water (UNADW). The whole area is affected by strong diapycnal turbulent mixing of the lower thermocline waters [*St. Laurent and Thurnherr*, 2007]. Located further south than 40°N, far from active deep-water formations areas associated with large flux of atmospheric ^{14}C to the surface waters, MD95-2037 is less likely to be affected by large variations in surface reservoir age [*Waelbroeck et al.*, 2001]. The age model was built using 9 AMS ^{14}C ages, converted in calendar ages using Calib Radiocarbon calibration program 5.1 [*Stuiver et al.*, 1998], after correction of a constant reservoir age of 400 years (Figure 2a and Table 3). The core was studied at high resolution along the glacial-interglacial transition (every 1–5 cm representing approximately 100–500 year resolution), particularly around H1 and YD (every centimeter representing less than 50 years resolution).

4. Results

[17] Only the new cores profiles will be presented in detail, and we refer to *Gherardi et al.* [2005], *McManus et al.* [2004], and *Hall et al.* [2006] for presentation of SU81-18, GGC5 and DAPC2 Pa/Th results respectively. In our discussion, however, the new results are compared to the published ones. To do so, time slices have been defined, and average sedimentary Pa/Th have been calculated for each of these time slices and for each cores (see Table 4): LGM (21–18 ka) [*Bard*, 1999], H1 (17–15 ka) [*Bard et al.*, 2000], BA (14.5–13 ka) [*Bard et al.*, 1996; *Weaver et al.*, 2003], YD (12.8–11.6 ka) [*Taylor et al.*, 1997], and the upper Holocene (8–0 ka).

4.1. Deep Cores

4.1.1. SU90-44

[18] Pa/Th variations in SU90-44 are similar to GGC5 and SU81-18 through the transition from H1 to BA (Figures 3c, 3d, and 3e). The three profiles have high Pa/Th during H1, followed by a decrease at the onset of the BA. The abrupt H1-BA transition in SU90-44 is well resolved by close sampling in this interval, and coincides with a late maximum in the IRD peak that defines H1 (Figure 2c). The low sedimentation rate of this core (less than 5 cm/ka), and lower sampling resolution did not capture the YD event. The profiles show also a gradual Pa/Th decrease toward Holocene values, similar to GGC5. During the LGM, however, the Pa/Th in this core diverges from the other two records. In particular, the mean LGM Pa/Th for SU90-44 (Pa/Th_{LGM} = 0.079 (±0.004, 2σ, n = 3)) is noticeably higher than for SU81-18 (Pa/Th_{LGM} = 0.049 (±0.002, 2σ, n = 6)) These two cores come from the same basin, but the latter was taken at shallower depth and at lower latitude.

4.1.2. MD95-2027

[19] Sedimentary Pa/Th during the LGM-H1 transition obtained from core MD95-2027 off Newfoundland, although somewhat scattered, shares some similarities with the other deep site from the western basin (Bermuda rise core GGC5) but the data have larger error bars and are more scattered (Figure 3e). The very large error bars observed during the first half of H1 (larger than 0.008, 2σ) (Figure 3e) are due to high IRD content, which lowers drastically the concentration of $^{230}Th_{ex}$ and $^{231}Pa_{ex}$ in these samples (Figures 2b and 4b). These levels are excluded from the discussion. During the LGM, MD95-2027 Pa/Th ratios are higher than in core GGC5, further south (Pa/Th_{LGM} = 0.080 ± 0.003, 2σ, n = 4, for MD95-2027, and Pa/Th_{LGM} = 0.068 ± 0.010.2σ, n = 12 for GGC5), but the statistical significance of this difference needs confirmation. Abrupt increase toward the production rate occurs during the second half of H1. This transition is well defined by a large IRD peak reaching a maximum at 16 ka (Figures 2b and 4b). The ''Heinrich'' mean ratio is the same for both deep western cores, (Pa/Th_{H1} = 0.083 (±0.008, 2σ, n = 9) excluding the levels with large error bars corresponding to the maximum content in IRD), for MD95-2027, versus Pa/Th_{H1} = 0.083

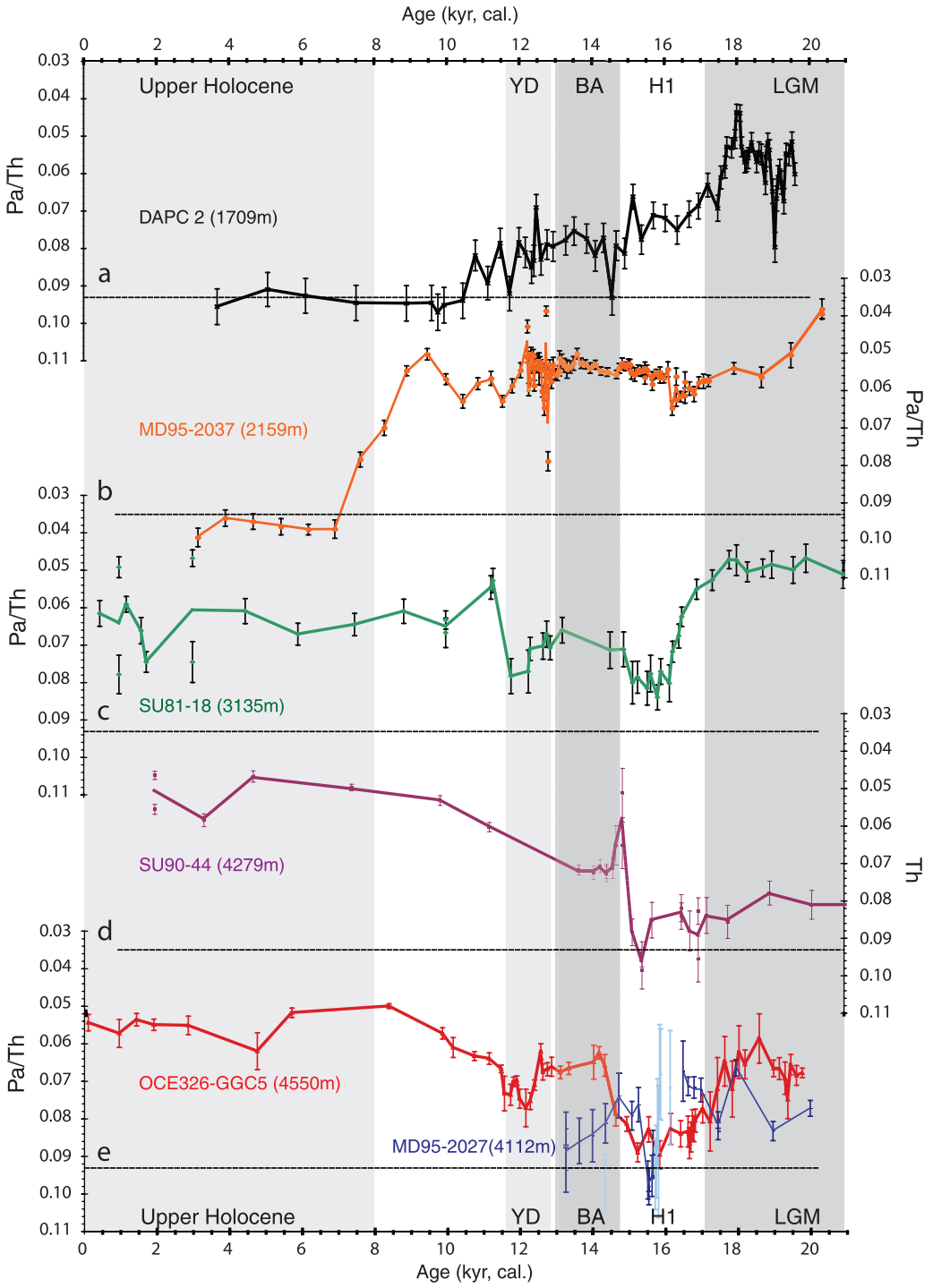

Figure 3. Sedimentary $^{231}Pa/^{230}Th$ signals; cores have been ordered by depth, except from MD95-2027 directly compared to GGC5 because of its close vicinity. (a) DAPC2 Pa/Th record [*Hall et al.*, 2006], (b) MD95-2037 Pa/Th record, (c) SU81-18 [*Gherardi et al.*, 2005] Pa/Th record, (d) SU90-44 sedimentary Pa/Th signal, and (e) OCE326-GGC5 (thick red curve) [*McManus et al.*, 2004] compared with MD95-2027 (thin blue curve). The $^{231}Pa/^{230}Th$ scale is inverted. The same vertical scale is used. Dashed lines stand for the production rate (0.093) [*Yu et al.*, 1996]. Standard errors are shown at 2σ. All of the MD95-2037 signal has been smoothed using a three-point moving average. Light blue points with light blue error bars are the reliable analytical points not taken into account for the final signal because of a high error bar (>0.008, 2σ) for MD95-2027.

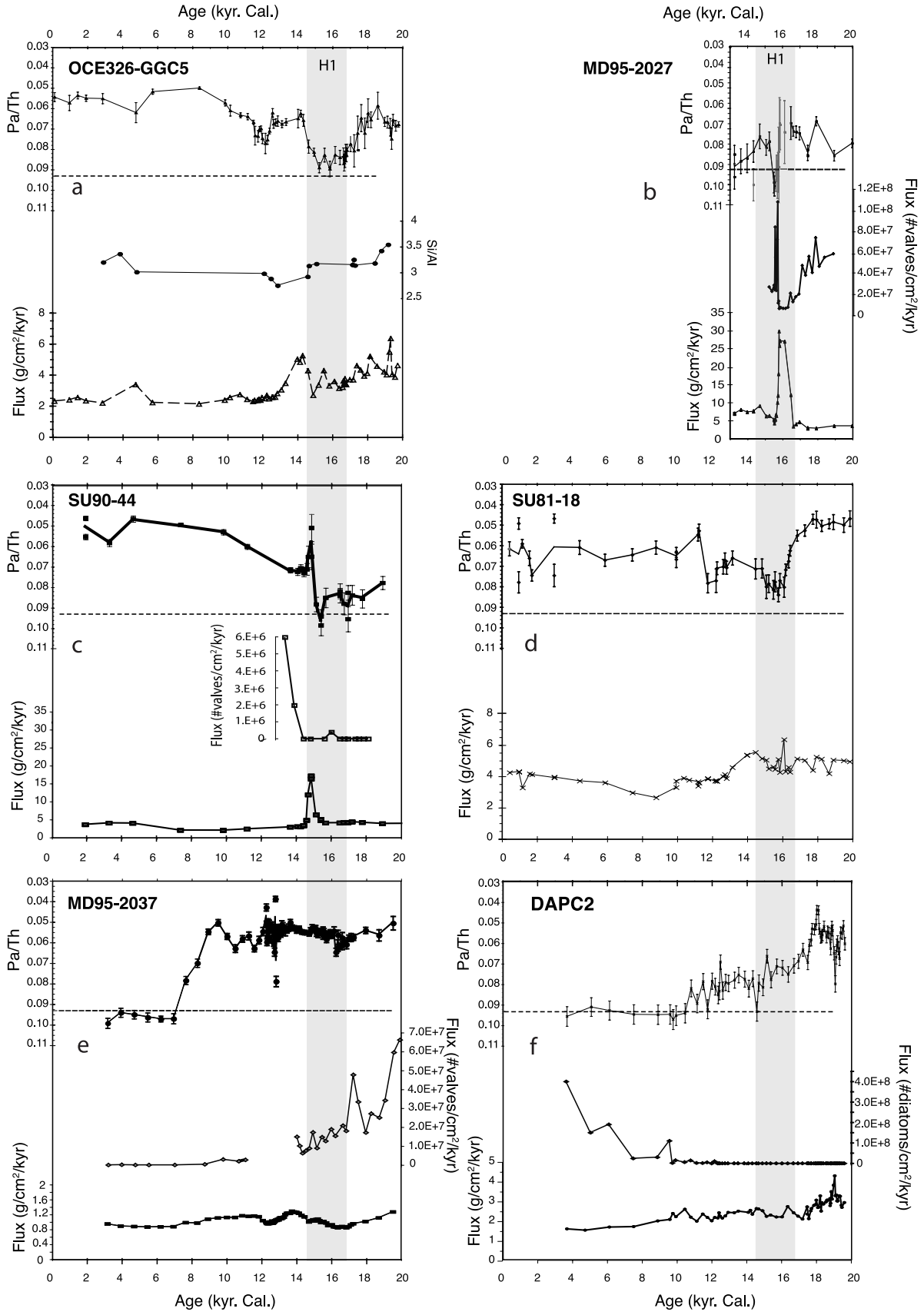
OCE326-GGC5
H1
a
Pa/Th
Si/Al
Flux (g/cm²/kyr)
MD95-2027
b
Flux (#valves/cm²/kyr)
SU90-44
c
Flux (#valves/cm²/kyr)
SU81-18
d
MD95-2037
e
DAPC2
f
Flux (#diatoms/cm²/kyr)
Age (kyr. Cal.)

Figure 4

(±0.004, 2σ, n = 16) for GGC5). The main difference between the two records occurs during the BA. MD95-2027 presents increasing Pa/Th value, with a mean of 0.085 (±0.006, 2σ, n = 6), whereas GGC5 is characterized by decreasing values toward 0.065.

4.2. Intermediate Depth Cores

[20] The shallowest cores present a Pa/Th signal drastically different from the deep cores (Figures 3a and 3b). In both DAPC2 and MD95-2037, the LGM period is characterized by low Pa/Th (0.053 (±0.002, 2σ, n = 16) and 0.046 (±0.008, 2σ, n = 4) respectively), while values close to the production rate ratios are found during the upper Holocene. The main difference between the two records is a gradual increase in Pa/Th in the northern core, contrasting with the stepwise changes found at lower latitude. DAPC2 also reaches the production rate ratio earlier (10 ka BP) than MD95-2037 (7 ka BP). This time lag difference is most likely due to a lack of time constrains during this transition since DAPC2 is characterized by only 2 ^{14}C AMS dates at 9.2 and 11.8 ka [*Hall et al.*, 2006; *Knutz et al.*, 2002] and MD95-2037 has dates only at 6 and 10 ka (Table 3).

[21] In the mid-Atlantic ridge core MD95-2037, we do not find significant changes in Pa/Th corresponding to the abrupt changes characterizing the deglaciation in the deeper records. The Pa/Th mean during the deglaciation (Pa/Th_{deg} = 0.056 (±0.001, 2σ, n = 81), from 18.5 to 10 ka) is similar to the ratio defining the Holocene period of the deep Atlantic cores (Pa/Th_{Hol} = 0.055 (±0.002, 2σ, n = 8) for GGC5 [*McManus et al.*, 2004]; Pa/Th_{Hol} = 0.064 (±0.003, 2σ, n = 11) for SU81-18 [*Gherardi et al.*, 2005]; and Pa/Th_{Hol} = 0.052 (±0.006, 2σ, n = 5) for SU90-44). This suggests an important renewal of the water masses bathing the first 2000 m of the North Atlantic ocean during the entire time period.

5. Discussion

5.1. Effect of Particle Flux and Composition

[22] As indicated earlier, the interpretation of the sedimentary Pa/Th ratio in terms of overturning rates can be biased by variations in particle flux and composition [*Anderson et al.*, 1983a; *Chase et al.*, 2002]. Because of this caveat the use of Pa/Th as a paleocirculation proxy has recently been challenged [*Keigwin and Boyle*, 2008; *Scholten et al.*, 2008]. It is therefore important to address this concern when discussing the new profiles.

5.1.1. Deep Cores

[23] Normalized ^{230}Th fluxes method [*Francois and Bacon*, 1994] have been used to show that massive increase in detrital fluxes occurred during the Heinrich event H1 within the zone of maximum IRD input, the so-called Ruddiman zone [*Grousset et al.*, 1993] (Figures 4b and 4c, bottom curves (cores MD95-2027 and SU90-44)). Total fluxes increased by about a factor of 4 in core SU90-44 during H1, but Pa/Th ratios remain low (Pa/Th values between 0.051 and 0.065). Instead, high Pa/Th ratios observed prior to this period of high flux are associated with comparatively low flux. Likewise diatoms are absent or in very low abundance for the LGM-H1 transition when Pa/Th is relatively high and increase at the end of the cold event (Figure 4c, middle curve) [*Nave et al.*, 2007] after Pa/Th has reached lower values. Clearly the Pa/Th record in this core cannot be explained by variations in particle flux and composition.

[24] In core MD95-2027, total sedimentary fluxes (Figure 4b, bottom curve) increase by about a factor 6 during H1. Deglacial fluxes in core MD95-2027 are higher than during glacial. This can be attributed to the vicinity of the Laurentide ice sheet, and its progressive melting during the deglaciation. Pa/Th in this profile is also higher during the deglaciation than during the LGM. The increasing Pa/Th during BA coincides with higher total mass fluxes (Figure 4b, top and bottom curves). Therefore, we cannot rule out enhanced Pa scavenging due to higher sedimentary flux at this site at the end of H1 and the onset of the warm Bølling-Allerød. Diatom fluxes decrease drastically at the onset of H1, because of a drop in primary productivity [*Nave et al.*, 2007], and increase again after the IRD peak (Figure 4b, middle curve). Higher diatom fluxes also coincide with Pa/Th ratios approaching the production rate, although these data have high error bars because of high IRD content. High diatoms fluxes following the IRD peak ($\sim 2*10^7$ #valves/cm^2/ka) coincide with Pa/Th ratios going from the production rate to lower values. Thus, this record indicates that the link between opal abundance and Pa scavenging is complex. The Pa/Th record of this core is nonetheless a useful illustration of the limitation of Pa/Th as a paleocirculation proxy. In this case we cannot clearly distinguish between the effect of particle scavenging and circulation and data from this core are not considered further.

[25] Evidently, variable sedimentary Pa/Th can only be taken as indicative for changes in the meridional circulation when particle flux and composition either remain constant, (i.e., when the fractionation between the two radionuclides remains relatively constant [*Scholten et al.*, 2008]) or change in a pattern inconsistent with Pa/Th variability. Therefore the transition from LGM to H1 in cores GGC5 and SU90-44, characterized by a progressive increase of the sedimentary Pa/Th and relatively constant fluxes (Figures 4a and 4c), can be interpreted in terms of a strong weakening of the meridional circulation [*McManus et al.*, 2004]. In the Iberian margin core SU81-18, the total mass flux is relatively constant during this transition and it has been demonstrated that diatom productivity decreased to a very low level during the deglaciation in this region [*Abrantes*, 2000]. Therefore the interpretation of the increasing Pa/Th ratio in terms of a slowdown of the circulation is also robust for this site [*Gherardi et al.*, 2005]. The same observation can be made for the transition from the warm BA to the Holocene at these sites, supporting the interpretation of another slowing

Figure 4. Comparison of sedimentary data: sedimentary Pa/Th signal (top curves), total diatom fluxes (in number of valves/cm^2/ka; middle curves) when available and Si/Al ratio for OCE326-GGC5, and total ^{230}Th-normalized flux of sediment (in g/cm^2/ka; bottom curves) for all cores versus calendar ages. (a) OCE326-GGC5 [*McManus et al.*, 2004], (b) MD95-2027, (c) SU90-44, (d) SU81-18 [*Gherardi et al.*, 2005], (e) MD95-2037, and (f) DAPC2 [*Hall et al.*, 2006].

down of the circulation during YD (Figures 4a, 4c, and 4d) and a resumption of the circulation at the onset of the Holocene.

5.1.2. Intermediate Depth Core

[26] For the central North Atlantic intermediate core MD95-2037, ^{230}Th-normalized total mass flux does not vary significantly during the deglaciation, in agreement with the location of the core within the oligotrophic zone of the subtropical gyre (Figure 4e, bottom curve). Fluxes of diatoms tests gradually decrease from the LGM through the deglaciation to reach values close to zero during the early Holocene. Pa/Th remains constant as opal flux decrease and increases to production rate ratio well after diatom valve numbers drop to zero. There is therefore no evidence for enhanced scavenging due to opal or particle flux throughout the study interval. Likewise, the high Pa/Th values found in the upper Holocene of core MD95-2037 cannot be attributed to its proximity with the Lucky Strike hydrothermal field. Higher hydrothermal activity could result in higher oxide concentration in sediments. Just like opal, Fe and Mn oxides have higher affinity for Pa and higher concentration of oxides in sediment would result in higher Pa/Th [*Chase et al.*, 2002]. However, we could not detect any significant increase in oxide deposition during the late Holocene in this core, as evidenced by Fe/^{232}Th or Mn/^{232}Th, (see Figure S1 in the auxiliary material). This observation provides additional support for the interpretation of Pa/Th in terms of intermediate water circulation changes.

[27] For the shallowest core, DAPC2, from the Rockall trough, *Hall et al.* [2006] have suggested that the high Pa/Th ratio characterizing the Holocene part of their record results from the high opal flux to sediment at this site. However, a similar level of opal abundance is reached during the LGM in core MD95-2037, with no influence on the glacial Pa/Th record, casting doubt on this explanation.

[28] In their recent work in the Southeastern Atlantic, *Scholten et al.* [2008] have also demonstrated that the shallowest cores (below 2000 m) are more likely sensitive to particles fluxes due to changes in the fractionation between ^{231}Pa and ^{230}Th toward lower value; therefore, the production ratio characterizing the upper Holocene at DAPC2 site, could be a combined effect of decreased circulation and increased opal flux.

[29] The production rate reached at both shallower sites during the upper Holocene indicate that the export of intermediate waters out of the northern Atlantic decreased several thousand years ago to values exceeding by about a factor three or more the residence time of ^{231}Pa in these waters, consistent with dissolved CO2 Δ^{14}C values measured at about 1000 m water depth further to the west [*Broecker and Peng*, 1982; *Campin et al.*, 1999]. Water column profiles of dissolved ^{230}Th [*Marchal et al.*, 2007], and ^{231}Pa R. Francois, unpublished data, 2008) follows a nearly linear trend with respect to depth specifically on the upper depth range (down to 2500 m), and can be predicted by a simple reversible scavenging model which neglects advection and diffusion [*Marchal et al.*, 2007]. Unlike during the LGM and the deglaciation, the residence time of intermediate water in the North Atlantic during the Holocene is sufficiently long to prevent significant export of ^{231}Pa by circulation. This also suggests that during the LGM and the deglaciation the residence time of intermediate water must have been quite short to allow important export of ^{231}Pa as suggested by profiles from DAPC2 and MD95-2037.

[30] It is clear that most of the Pa/Th profiles reported here cannot be readily explained by changes in particle flux or composition. Therefore, changes in the rate of overturning circulation seem the only remaining explanation. In the following, we further support this conclusion by showing the coherence of the Pa/Th records obtained from different depths and how consistent the bathymetric profiles in Pa/Th are with our understanding of ocean circulation.

5.2. Renewal Rates of Deep and Intermediate Water Masses: Time Slices

[31] To better extract the information on circulation changes associated with the climatic events affecting the deglaciation, we have calculated the mean sedimentary Pa/Th ratios in each core for the five different time slices defined previously (LGM, H1, BA, YD, and upper Holocene) and plotted them against water depth (Figure 5 and Table 4).

5.2.1. Upper Holocene

[32] The Holocene profile shows an decreasing trend with depth (Figure 5a, orange curve), in agreement with observations [*Bryden et al.*, 2005; *Smethie and Fine*, 2001] and model results [*Böning et al.*, 1995] indicating a vigorous export of North Atlantic deep water (deeper than about 2500 m), and a weaker intermediate water export. This observation lends support to the interpretation of the other time slices in terms of circulation changes.

[33] The cores collected below 4000 m depth could also be influenced by Antarctic Bottom water (AABW). In the modern ocean, however, the AABW is believed to have little impact on the Pa/Th of North Atlantic sediments. This is because (1) AABW rate of formation is small compared to that of the NADW, (2) AABW occupies only a small depth interval of the water column, and (3) the initial ^{230}Th and ^{231}Pa concentration in the AABW is relatively high. Significant export of ^{231}Pa from the southern ocean to the North Atlantic with AABW would require initial dissolved ^{230}Th and ^{231}Pa concentrations well below their concentration in equilibrium with respect to scavenging at the final depth of lateral transport, thereby allowing for a gradual increase in dissolved ^{231}Pa concentration along the northward path of the AABW. Because of deep convection mixing and relatively low scavenging intensity in the Weddell Sea, surface and intermediate depth waters that produce AABW have high initial concentrations [e.g., *Rutgers van der Loeff and Berger*, 1993] allowing for only a small increment in concentration as AABW flows northward, thereby severely limiting its ''carrying capacity'' for ^{231}Pa. We believe that we can therefore safely neglect the potential imprint of AABW in the Holocene portion of this study, although the exact influence of AABW on Pa/Th in Atlantic sediment needs to be further clarified. In particular, AABW likely contributes to the low Pa/Th found in the sediment of the south Atlantic (Y. Luo, unpublished data,

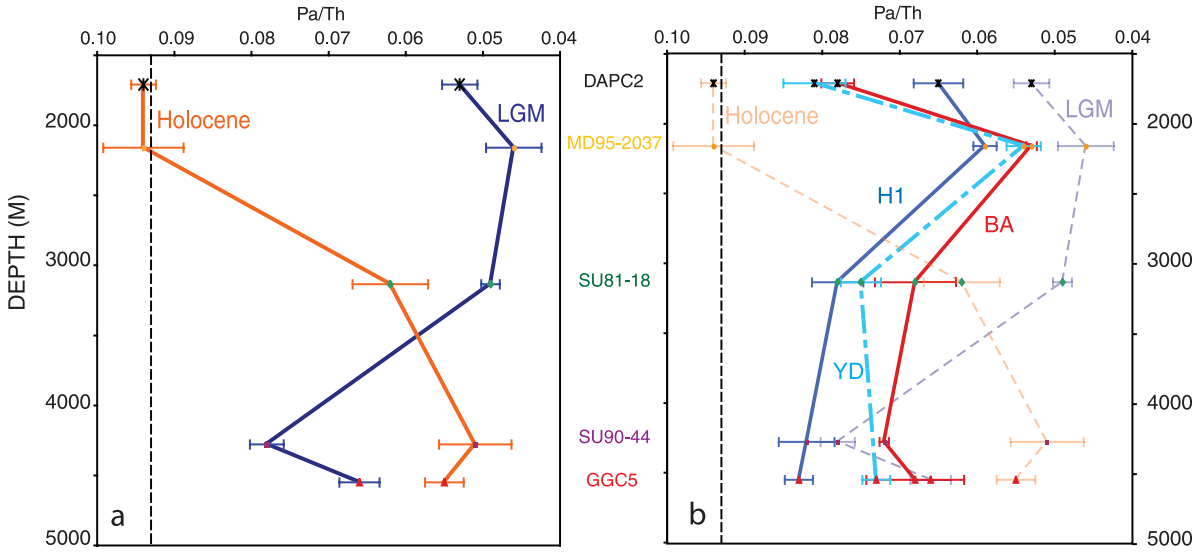

Figure 5. Sedimentary $^{231}Pa/^{230}Th$ time slices versus water depth. (a) LGM (solid dark blue) versus Holocene (orange) time slice. (b) H1 (solid dark blue), BA (red), and YD (dash-dotted light blue). LGM and Holocene (dashed dark blue and dashed orange, respectively) are maintained for comparison. The $^{231}Pa/^{230}Th$ scale is inverted in order to show strong MOC on the right-hand side and a reduced one on the left-hand side of Figures 5a and 5b (production rate is represented by the black dashed line).

2008) which could possibly provide constraints on past changes in the rate of AABW formation.

5.2.2. LGM

[34] During the LGM (Figure 5a, dark blue curve), Pa/Th shows a clear increasing trend with depth, in agreement with a rapid overturning at intermediate depths associated with the GNAIW [*Boyle and Keigwin*, 1987; *Duplessy et al.*, 1988; *Oppo and Fairbanks*, 1987; *Sarnthein et al.*, 1994], and a decrease or disappearance of the lower NADW. The shift in the Pa/Th bathymetric profile between the Holocene and the LGM (Figure 5a) is consistent with the two different circulation modes previously inferred from nutrient proxies [*Curry and Oppo*, 2005; *Labeyrie et al.*, 1992] and further supports our interpretation of Pa/Th as a paleocirculation tracer.

[35] The data indicate a very vigorous circulation at intermediate depth during the LGM, which reached at least 3000 m depth in the eastern basin because Pa/Th in SU81-18 records significant export of ^{231}Pa in the overlying water column. This corroborates earlier suggestions that the LGM may have been characterized by a substantial overturning circulation that was restricted to intermediate depths [*Curry and Mauritzen*, 2005; *Gherardi et al.*, 2005; *McManus et al.*, 2004] and is also in line with models suggesting that the total overturning may have even been stronger during the LGM [*Roche et al.*, 2007]. In contrast, the deep waters were clearly less actively renewed and poorly ventilated [*Labeyrie et al.*, 2005]. Nonetheless, LGM Pa/Th ratios in the two deeper cores are significantly less than the production ratio. These values may be an attenuated signal of the shallow overturning. The low Pa/Th imparted to settling particles by a shallow overturning cell propagates downward as a result of reversible adsorption of ^{231}Pa and ^{230}Th on particles. The signal is however quickly attenuated with increasing depth and it has been argued that sediment Pa/Th only records overturning cells occurring within ~1000 m of the seafloor [*Thomas et al.*, 2006]. Whether the deep water LGM Pa/Th in the North Atlantic is (1) an attenuated signal of the northern source shallow overturning cell or (2) an attenuated signal of a southern source overturning cell still needs to be established.

[36] While the intermediate depth cores of this study have probably been bathed by a northern component water mass throughout the time span of interest, nutrient tracers indicate that below 2500–3000 m the north Atlantic was filled with a nutrient rich southern component water mass [*Lynch-Stieglitz et al.*, 2007]. Therefore the question of the influence of southern water on Pa/Th in the deeper cores remains to be investigated. Preliminary results from a 2-D circulation-scavenging model (Luo et al., unpublished data, 2008) indicate that the formation of AABW is critical for producing low Pa/Th in the south Atlantic, north of the Polar Frontal Zone. And yet, the northern source overturning cell is believed to have little impact on the Pa/Th of the south Atlantic [*Marchal et al.*, 2001], to the same extent, enhanced northward penetration of AABW may have had little impact on the sediment of the North Atlantic. If there is transport of ^{231}Pa from the southern ocean into the North Atlantic during the LGM, that would require an even more effective southward export of ^{231}Pa by an even faster GNAIW to account for the North Atlantic Pa/Th record. Quantifying this effect, however, still requires a detailed sedimentary Pa/Th record from the South Atlantic.

5.2.3. Heinrich Event H1

[37] The cold event occurring at the early stage of the deglaciation appears to be associated with the most drastic

reduction in the rate of deep-water overturning [*Gherardi et al.*, 2005; *McManus et al.*, 2004]. The bathymetric Pa/Th profile obtained during H1 (Figure 5b, solid dark blue curve) is characterized by a general increase in Pa/Th compared to the LGM profile, which can be taken as reflecting a general decrease in the rate of overturning at all depths. There is, however, clear evidence for continued, if slower, overturning down to 2000 m depth. This is in agreement with *Labeyrie et al.* [2005], who interpreted the decrease in $\delta^{13}C$ during H1 in the North Atlantic as a result of the formation of shallower intermediate water, produced by brine ejection and depleted in ^{13}C. Our earlier interpretation of the GGC5 profile as reflecting a near total shutdown of the North Atlantic overturning circulation during H1 must therefore be revised. Although the ''Heinrich mode'' of deep water circulation is characterized by dramatically reduced deep water renewal rates, there was still an active shallow overturning cell that was exporting water and ^{231}Pa from the North Atlantic.

5.2.4. BA

[38] This period is commonly thought to have had a circulation mode similar to the modern ocean, with active deep NADW formation, and weaker or no intermediate water formation [*Broecker and Denton*, 1989; *Sarnthein et al.*, 1994, 1995]. However, the Pa/Th bathymetric profile obtained for that period suggests a circulation mode very different from the upper Holocene and intermediate between the more active LGM overturning and the slower overturning associated with H1 (Figure 5b, red curve). The profile suggests moderate export at all depths, rather than the apparent LGM-Holocene tradeoff between intermediate and deep export. This is in agreement with a recent study based on $\varepsilon_{(Nd)}$ in the drift deposit accumulating on Black Ridge [*Gutjahr et al.*, 2008] which suggests that the modern circulation pattern was initiated after the Younger Dryas.

5.2.5. YD

[39] The depth transect for the Younger Dryas time slice (Figure 5b, dash-dotted light blue curve) is constrained only by two deep cores, SU81-18 at 3135 m and GGC5 at 4550 m. The results suggest only a slight decrease of the deep water renewal rate below 3000 m compared to BA whereas the intermediate overturning at ~2000 m is maintained. The circulation characteristics of the YD appear to be intermediate between those of H1 and BA.

6. Conclusion

[40] This study further supports the potential of sedimentary Pa/Th in the North Atlantic for reconstructing past changes in Atlantic MOC. It also illustrates the conditions for which the interpretation of the Pa/Th ratio as a circulation tracer may be obscured by changes in particle scavenging. By compiling the Pa/Th ratios in cores at different depth we are able to better constrain changes in the rate of formation of the main water masses. Particularly, the focus on two intermediate depth cores from the mid-Atlantic ridge and the Rockall Trough provides evidence for rapid intermediate water overturning during the LGM. This intermediate overturning cell shoaled and slowed but remained active during H1, BA, and YD, hence, a significant MOC at intermediate depths characterized the entire deglacial interval. In deeper water, MOC was significantly reduced during the LGM and deglaciation compared to present and accelerated after the YD The Holocene Pa/Th bathymetric profile is consistent with a weaker overturning above ~2500 m and fast water renewal rates deeper, in agreement with modern observations. The LGM Pa/Th profile is also consistent with nutrient tracers. Our new results provide new insight into the Heinrich stadial circulation mode, which has been previously interpreted to be a total shut down of the MOC. Finally our results suggest, for the first time, that circulation during the BA was very different from the modern circulation, with a relatively weak overturning occurring both in intermediate and deep waters. This study further demonstrates the potential of Pa/Th as a paleocirculation tracer and indicates that as its spatial and bathymetric coverage increase, it will provide an increasingly detailed and accurate reconstruction of the glacial and deglacial circulation.

[41] **Acknowledgments.** The $^{231}Pa/^{230}Th$ measurements have been run at the Woods Hole Oceanographic Institution with funds from NSF grant OCE-0099176. Dave Schneider from the ICP-MS facility lab and Alan Fleer and Suzan Brown-Leger from the Geology and Geochemistry Department are acknowledged for their analytical and technical support. We thank G. Henderson, M. Siddall, and M. Rutgers van der Loeff for their review and comments that enhanced considerably the quality of this paper. The LSCE-WHOI cooperation has been supported by a NSF-CNRS cooperative grant NSF INT-0233483. Analytical measurements in LSCE have been supported by French Programme National d'Etude de la Dynamique du Climat, Commissariat à l'Energie Atomique, and Centre National de la Recherche Scientifique. Brigitte Lecoat and Jerôme Tessier are thanked for the analytical support, and Claire Waelbroeck is thanked for interactions during this work. Trond Dokken and Øyving Lie from BCCR are thanked for their support and fruitful comments on the manuscript. The participation of J.F.M. in this project was supported in part by grants from the U.S.-NSF, WHOI-OCCI, and the Gary Comer Science and Education Foundation. R.F.'s participation was supported by grants from NSERC and the Canadian Foundation for Climate and Atmospheric Science. This is publication A 206 from the Bjerknes Centre for Climate Research.

References

Abrantes, F. (2000), 200 000 yr diatom records from Atlantic upwelling sites reveal maximum productivity during LGM and a shift in phytoplankton community structure at 185 000 yr, *Earth Planet. Sci. Lett.*, *176*, 7–16, doi:10.1016/S0012-821X(99)00312-X.

Anderson, R. F., and A. P. Fleer (1982), Determination of natural actinides and plutonium in marine particulate material, *Anal. Chem.*, *54*, 1142–1147, doi:10.1021/ac00244a030.

Anderson, R. F., et al. (1983a), Removal of ^{230}Th and ^{231}Pa at ocean margin, *Earth Planet. Sci. Lett.*, *66*, 73–90, doi:10.1016/0012-821X(83)90127-9.

Anderson, R. F., et al. (1983b), Removal of ^{230}Th and ^{231}Pa from the open ocean, *Earth Planet. Sci. Lett.*, *62*, 7–23, doi:10.1016/0012-821X(83)90067-5.

Bacon, M. P. (1984), Glacial to interglacial changes in carbonate and clay sedimentation in the Atlantic Ocean estimated from ^{230}Th measurements, *Isot. Geosci.*, *2*, 97–111.

Bard, E. (1999), Ice age temperatures and geochemistry, *Science*, *284*, 1133–1134, doi:10.1126/science.284.5417.1133.

Bard, E., et al. (1996), Deglacial sea-level record from Tahiti corals and the timing of global meltwater discharge, *Nature*, *382*, 241–244, doi:10.1038/382241a0.

Bard, E., et al. (2000), Hydrological impact of Heinrich events in the sub-tropical northeast Atlantic, *Science*, *289*, 1321–1324, doi:10.1126/science.289.5483.1321.

Böning, C. W., et al. (1995), An overlooked problem in model simulations of the thermohaline circulation and heat transport in the Atlantic Ocean, *J. Clim.*, *8*, 515–523, doi:10.1175/1520-0442(1995)008<0515:AOPIMS>2.0.CO;2.

Boyle, E. A., and L. Keigwin (1987), North Atlantic thermohaline circulation during the past 20,000 years linked to high latitude surface temperature, *Nature*, *330*, 35–40, doi:10.1038/330035a0.

Broecker, W. S. (1979), A revised estimate for the radiocarbon age of North Atlantic deep water, *J. Geophys. Res.*, *84*, 3218–3226, doi:10.1029/JC084iC06p03218.

Broecker, W. S., and G. H. Denton (1989), The role of ocean-atmosphere reorganizations in glacial cycles, *Geochim. Cosmochim. Acta*, *53*, 2465–2501, doi:10.1016/0016-7037(89)90123-3.

Broecker, W. S., and T.-H. Peng (1982), *Tracers in the Sea*, Columbia Univ. Press, Palisades, N. Y.

Bryden, H. L., et al. (2005), Slowing of the Atlantic meridional overturning circulation at 25°N, *Nature*, *438*, 655–657, doi:10.1038/nature04385.

Calvo, E., et al. (2001), New insights into the glacial latitudinal temperature gradients in the North Atlantic: Results from $U^{k'}_{37}$ sea surface temperatures and terrigenous inputs, *Earth Planet. Sci. Lett.*, *188*, 509–519, doi:10.1016/S0012-821X(01)00316-8.

Came, R. E., D. W. Oppo, W. B. Curry, and J. Lynch-Stieglitz (2008), Deglacial variability in the surface return flow of the Atlantic meridional overturning circulation, *Paleoceanography*, *23*, PA1217, doi:10.1029/2007PA001450.

Campin, J. M., et al. (1999), Problems with using radiocarbon to infer ocean ventilation rates for past and present climates, *Earth Planet. Sci. Lett.*, *165*, 17–24, doi:10.1016/S0012-821X(98)00255-6.

Chase, Z., R. F. Anderson, M. Q. Fleisher, and P. W. Kubik (2002), The influence of particle composition and particle flux on scavenging of Th, Pa and Be in the ocean, *Earth Planet. Sci. Lett.*, *204*, 215–229, doi:10.1016/S0012-821X(02)00984-6.

Chase, Z., et al. (2003), Scavenging of ^{230}Th, ^{231}Pa and ^{10}Be in the Southern Ocean (SW Pacific sector): The importance of particle flux, particle composition and advection, *Deep Sea Res., Part II*, *50*, 739–768, doi:10.1016/S0967-0645(02)00593-3.

Choi, M. S., R. Francois, K. Sims, M. P. Bacon, S. Brown-Leger, A. P. Fleer, L. Ball, D. Schneider, and S. Pichat (2001), Rapid determination of ^{230}Th and ^{231}Pa in seawater by desolvated micro-nebulization inductively coupled plasma magnetic sector mass spectrometry, *Mar. Chem.*, *76*, 99–112, doi:10.1016/S0304-4203(01)00050-0.

CLIMAP Project Members (1984), The last interglacial ocean, *Quat. Res.*, *21*, 123–224, doi:10.1016/0033-5894(84)90098-X.

Cortijo, E., et al. (1997), Changes in sea surface hydrology associated with Heinrich event 4 in the North Atlantic Ocean between 40° and 60°N, *Earth Planet. Sci. Lett.*, *146*, 29–45, doi:10.1016/S0012-821X(96)00217-8.

Curry, R., and C. Mauritzen (2005), Dilution of the northern North Atlantic Ocean in recent decades, *Science*, *308*, 1772–1774, doi:10.1126/science.1109477.

Curry, W. B., and D. W. Oppo (2005), Glacial water mass geometry and the distribution of δ^{13}C of ΣCO_2 in the western Atlantic Ocean, *Paleoceanography*, *20*, PA1017, doi:10.1029/2004PA001021.

Duplessy, J. C., N. J. Shackleton, R. G. Fairbanks, L. Labeyrie, D. Oppo, and N. Kallel (1988), Deepwater source variations during the last climatic cycle and their impact on the global deepwater circulation, *Paleoceanography*, *3*, 343–360, doi:10.1029/PA003i003p00343.

Francois, R., and M. P. Bacon (1994), Heinrich events in the North Atlantic: Radiochemical evidence, *Deep Sea Res., Part I*, *41*, 315–334, doi:10.1016/0967-0637(94)90006-X.

Francois, R., M. Frank, M. M. Rutgers van der Loeff, and M. P. Bacon (2004), ^{230}Th normalization: An essential tool for interpreting sedimentary fluxes during the late Quaternary, *Paleoceanography*, *19*, PA1018, doi:10.1029/2003PA000939.

Gebbie, G., and P. Huybers (2006), Meridional circulation during the Last Glacial Maximum explored through a combination of South Atlantic δ^{18}O observations and a geostrophic inverse model, *Geochem. Geophys. Geosyst.*, *7*, Q11N07, doi:10.1029/2006GC001383.

Geibert, W., and R. Usbeck (2004), Adsorption of thorium and protactinium onto different particle types: Experimental findings, *Geochim. Cosmochim. Acta*, *68*, 1489–1501, doi:10.1016/j.gca.2003.10.011.

Gherardi, J.-M., et al. (2005), Evidence from the northeastern Atlantic basin for variability in the rate of the meridional overturning circulation through the last deglaciation, *Earth Planet. Sci. Lett.*, *240*, 710–723, doi:10.1016/j.epsl.2005.09.061.

Gregory, J. M., et al. (2005), A model intercomparison of changes in the Atlantic thermohaline circulation in response to increasing atmospheric CO_2 concentration, *Geophys. Res. Lett.*, *32*, L12703, doi:10.1029/2005GL023209.

Grousset, F. E., L. Labeyrie, J. A. Sinko, M. Cremer, G. Bond, E. Cortijo, and S. Huon (1993), Patterns of ice-rafted detritus in the glacial North Atlantic (40–55°N), *Paleoceanography*, *8*, 175–211, doi:10.1029/92PA02923.

Gutjahr, M., et al. (2008), Tracing the Nd isotope evolution of North Atlantic deep and intermediate waters in the western North Atlantic since the Last Glacial Maximum from Blake Ridge sediments, *Earth Planet. Sci. Lett.*, *266*, 61–77, doi:10.1016/j.epsl.2007.10.037.

Hall, I. R., S. B. Moran, R. Zahn, P. C. Knutz, C.-C. Shen, and R. L. Edwards (2006), Accelerated drawdown of meridional overturning in the late-glacial Atlantic triggered by transient pre-H event freshwater perturbation, *Geophys. Res. Lett.*, *33*, L16616, doi:10.1029/2006GL026239.

Henderson, G. M., and R. F. Anderson (2003), The U-series toolbox for paleoceanography, in *Uranium-Series Geochemistry*, *Rev. Mineral. Geochem.*, vol. 52, edited by B. Bourdon et al., pp. 493–531, Mineral. Soc. of Am., Washington, D. C.

Henderson, G. M., et al. (1999), Global distribution of the ^{230}Th flux to ocean sediments constrained by GCM modelling, *Deep Sea Res., Part I*, *46*, 1861–1893, doi:10.1016/S0967-0637(99)00030-8.

Hoffmann, S., and J. McManus (2007), Is there a ^{230}Th deficit in Arctic sediments?, *Earth Planet. Sci. Lett.*, *258*, 516–527, doi:10.1016/j.epsl.2007.04.011.

Keigwin, L. D., and E. A. Boyle (2008), Did North Atlantic overturning halt 17000 years ago?, *Paleoceanography*, *23*, PA1101, doi:10.1029/2007PA001500.

Keigwin, L. D., and M. A. Schlegel (2002), Ocean ventilation and sedimentation since the glacial maximum at 3 km in the western North Atlantic, *Geochem. Geophys. Geosyst.*, *3*(6), 1034, doi:10.1029/2001GC000283.

Knutz, P. C., et al. (2002), Multidecadal ocean variability and NW European ice sheet surges during the last deglaciation, *Geochem. Geophys. Geosyst.*, *3*(12), 1077, doi:10.1029/2002GC000351.

Labeyrie, L. D., et al. (1992), Changes in the vertical structure of the North Atlantic Ocean between glacial and modern times, *Quat. Sci. Rev.*, *11*, 401–413, doi:10.1016/0277-3791(92)90022-Z.

Labeyrie, L., H. Leclaire, C. Waelbroeck, E. Cortijo, J.-C. Duplessy, L. Vidal, M. Elliot, B. Le Coat, and G. Auffret (1999), Temporal variability of the surface and deep waters of the north West Atlantic Ocean at orbital and millennial scales, in *Mechanisms of Global Climate Change at Millennial Time Scales*, *Geophys. Monogr. Ser.*, vol. 112, edited by P. U. Clark, R. S. Webb, and L. D. Keigwin, pp. 77–98, AGU, Washington, D. C.

Labeyrie, L., et al. (2005), Changes in deep water hydrology during the last deglaciation, *C. R. Geosci.*, *337*, 919–927, doi:10.1016/j.crte.2005.05.010.

Legrand, P., and C. Wunsch (1995), Constraints from paleotracer data on the North Atlantic circulation during the Last Glacial Maximum, *Paleoceanography*, *10*, 1011–1045, doi:10.1029/95PA01455.

Lynch-Stieglitz, J., T. F. Stocker, W. S. Broecker, and R. G. Fairbanks (1995), The influence of air-sea exchange on the isotopic composition of oceanic carbon: Observation and modeling, *Global Biogeochem. Cycles*, *9*, 653–665, doi:10.1029/95GB02574.

Lynch-Stieglitz, J., W. B. Curry, and N. Slowey (1999), A geostrophic transport estimate for the Florida Current from the oxygen isotope composition of benthic foraminifera, *Paleoceanography*, *14*, 360–373, doi:10.1029/1999PA900001.

Lynch-Stieglitz, J., et al. (2007), Atlantic meridional overturning circulation during the Last Glacial Maximum, *Science*, *316*, 66–69, doi:10.1126/science.1137127.

Mackensen, A., H.-W. Hubberten, T. Bickert, G. Fischer, and D. K. Fütterer (1993), The δ^{13}C in benthic foraminiferal tests of *Fontbotia Wuellerstorfi* (Schwager) relative to the δ^{13}C of dissolved inorganic carbon in Southern Ocean deep water: Implications for glacial ocean circulation models, *Paleoceanography*, *8*, 587–610, doi:10.1029/93PA01291.

Marchal, O., R. Francois, T. F. Stocker, and F. Joos (2000), Ocean thermohaline circulation and sedimentary ^{231}Pa/^{230}Th ratio, *Paleoceanography*, *15*, 625–641, doi:10.1029/2000PA000496.

Marchal, O., T. F. Stocker, and R. Muscheler (2001), Atmospheric radiocarbon during the Younger Dryas: Production, ventilation, or both?, *Earth Planet. Sci. Lett.*, *185*, 383–395, doi:10.1016/S0012-821X(00)00383-6.

Marchal, O., et al. (2007), Contribution of ^{230}Th measurements to the estimation of the abyssal circulation, *Deep Sea Res., Part I*, *54*, 557–585, doi:10.1016/j.dsr.2007.01.002.

Marchitto, T. M., Jr., W. B. Curry, and D. W. Oppo (2000), Zinc concentrations in benthic foraminifera reflect seawater chemistry, *Paleoceanography*, *15*, 299–306, doi:10.1029/1999PA000420.

McManus, J. F., et al. (1998), Radiometrically determined sedimentary fluxes in the sub-polar North Atlantic during the last 140,000 years, *Earth Planet. Sci. Lett.*, *155*, 29–43, doi:10.1016/S0012-821X(97)00201-X.

McManus, J. F., et al. (2004), Collapse and rapid resumption of Atlantic meridional circulation linked to deglacial climate changes, *Nature*, *428*, 834–837, doi:10.1038/nature02494.

Nave, S., L. Labeyrie, J. Gherardi, N. Caillon, E. Cortijo, C. Kissel, and F. Abrantes (2007), Primary productivity response to Heinrich events in the North Atlantic Ocean and Norwegian Sea, *Paleoceanography*, *22*, PA3216, doi:10.1029/2006PA001335.

Nozaki, Y., and T. Nakanishi (1985), ^{231}Pa and ^{230}Th profiles in the open ocean water column, *Deep Sea Res., Part A*, *32*, 1209–1220, doi:10.1016/0198-0149(85)90004-4.

Oppo, D. W., and R. G. Fairbanks (1987), Variability in the deep and intermediate water circulation of the Atlantic Ocean during the last 25000 years: Northern Hemisphere modulation of the Southern Ocean, *Earth Planet. Sci. Lett.*, *86*, 1–15, doi:10.1016/0012-821X(87)90183-X.

Piotrowski, A. M., et al. (2004), Intensification and variability of ocean thermohaline circulation through the last deglaciation, *Earth Planet. Sci. Lett.*, *225*, 205–220, doi:10.1016/j.epsl.2004.06.002.

Robinson, L. F., et al. (2005), Radiocarbon variability in the western North Atlantic during the last deglaciation, *Science*, *310*, 1469–1473, doi:10.1126/science.1114832.

Roche, D. M., et al. (2007), Climate of the Last Glacial Maximum: Sensitivity studies and model-data comparison with the LOVECLIM coupled model, *Clim. Past*, *3*, 205–224.

Rutgers van der Loeff, M. M., and G. W. Berger (1993), Scavenging of ^{230}Th and ^{231}Pa near the Atlantic Polar Front in the South Atlantic, *Deep Sea Res., Part I*, *40*, 339–357, doi:10.1016/0967-0637(93)90007-P.

Sarnthein, M., K. Winn, S. J. A. Jung, J.-C. Duplessy, L. Labeyrie, H. Erlenkeuser, and G. Ganssen (1994), Changes in East Atlantic deepwater circulation over the last 30000 years: Eight time slice reconstructions, *Paleoceanography*, *9*, 209–267, doi:10.1029/93PA03301.

Sarnthein, M., et al. (1995), Variations in Atlantic surface ocean paleoceanography, 50°–80°N: A time-slice record of the last 30,000 years, *Paleoceanography*, *10*, 1063–1094, doi:10.1029/95PA01453.

Scholten, J. C., et al. (2008), Advection and scavenging: Effects on ^{230}Th and ^{231}Pa distribution off southwest Africa, *Earth Planet. Sci. Lett.*, *271*, 159–169, doi:10.1016/j.epsl.2008.03.060.

Schrader, H. J., and G. Schuette (1968), Marine diatoms, in *The Sea*, edited by C. Emiliani, pp. 1179–1231, John Wiley, New York.

Siddall, M., et al. (2005), ^{231}Pa/^{230}Th fractionation by ocean transport, biogenic particle flux and particle type, *Earth Planet. Sci. Lett.*, *237*, 135–155, doi:10.1016/j.epsl.2005.05.031.

Siddall, M., T. F. Stocker, G. M. Henderson, F. Joos, M. Frank, N. R. Edwards, S. P. Ritz, and S. A. Müller (2007), Modeling the relationship between ^{231}Pa/^{230}Th distribution in North Atlantic sediment and Atlantic meridional overturning circulation, *Paleoceanography*, *22*, PA2214, doi:10.1029/2006PA001358.

Smethie, W. M., and R. A. Fine (2001), Rates of North Atlantic deep water formation calculated from chlorofluorocarbon inventories, *Deep Sea Res., Part I*, *48*, 189–215, doi:10.1016/S0967-0637(00)00048-0.

St. Laurent, L. C., and A. M. Thurnherr (2007), Intense mixing of lower thermocline water on the crest of the Mid-Atlantic Ridge, *Nature*, *448*, 680–683, doi:10.1038/nature06043.

Stuiver, M., et al. (1998), INTCAL98 radiocarbon age calibration, 24,000–0 cal BP, *Radiocarbon*, *40*, 1041–1083.

Tachikawa, K., V. Athias, and C. Jeandel (2003), Neodymium budget in the modern ocean and paleo-oceanographic implications, *J. Geophys. Res.*, *108*(C8), 3254, doi:10.1029/1999JC000285.

Taylor, K. C., et al. (1997), The Holocene-Younger Dryas transition recorded at Summit, Greenland, *Science*, *278*, 825–827, doi:10.1126/science.278.5339.825.

Thomas, A. L., et al. (2006), Interpretation of the ^{231}Pa/^{230}Th paleocirculation proxy: New water-column measurements from the southwest Indian Ocean, *Earth Planet. Sci. Lett.*, *241*, 493–504, doi:10.1016/j.epsl.2005.11.031.

Turekian, K. K., and L. H. Chan (1971), The marine geochemistry of the uranium isotopes ^{230}Th and ^{231}Pa, in *Activation Analysis in Geochemistry and Cosmochemistry*, edited by A. O. Brunfelt and E. Steinnes, pp. 69–102, Oslo Univ. Press, Oslo.

Waelbroeck, C., et al. (2001), The timing of the last deglaciation in North Atlantic climate records, *Nature*, *412*, 724–727, doi:10.1038/35089060.

Waelbroeck, C., et al. (2006), Distant origin of circulation changes in the Indian Ocean during the last deglaciation, *Earth Planet. Sci. Lett.*, *243*, 244–251, doi:10.1016/j.epsl.2005.12.031.

Walter, H. J., et al. (1997), Enhanced scavenging of ^{231}Pa relative to ^{230}Th in the South Atlantic south of the Polar Front: Implications for the use of the ^{231}Pa/^{230}Th ratio as paleoproductivity proxy, *Earth Planet. Sci. Lett.*, *149*, 85–100, doi:10.1016/S0012-821X(97)00068-X.

Weaver, A. J., et al. (2003), Meltwater pulse 1A from Antarctica as a trigger of the Bølling-Allerød warm interval, *Science*, *299*, 1709–1713, doi:10.1126/science.1081002.

Wunsch, C. (2003), Determining paleoceanographic circulations, with emphasis on the Last Glacial Maximum, *Quat. Sci. Rev.*, *22*, 371–385, doi:10.1016/S0277-3791(02)00177-4.

Yu, E.-F., et al. (1996), Similar rates of modern and last-glacial ocean thermohaline circulation inferred from radiochemical data, *Nature*, *379*, 689–694, doi:10.1038/379689a0.

Yu, E.-F., et al. (2001), Fluxes of ^{230}Th, ^{231}Pa to the deep sea: Implications for the interpretation of excess ^{230}Th and ^{231}Pa/^{230}Th profiles in sediments, *Earth Planet. Sci. Lett.*, *191*, 219–230, doi:10.1016/S0012-821X(01)00410-1.

E. Cortijo and L. Labeyrie, Laboratoire des Sciences du Climat et de l'Environnement, CNRS, F-91190 Gif-sur-Yvette, France.

R. Francois, Department of Earth and Ocean Sciences, University of British Columbia, 6270 University Boulevard, Vancouver, BC V6T 1Z4, Canada.

J.-M. Gherardi, Bjerknes Center for Climate Research, University of Bergen, Allégaten 55, N-5007 Bergen, Norway. (jeanne.scao@bjerknes.uib.no)

J. F. McManus, Department of Geology and Geophysics, Woods Hole Oceanographic Institution, Woods Hole, MA 02543, USA.

S. Nave, Departamento de Geologia Marinha, Instituto Nacional de Engenharia, Tecnologia e Inovação, P-2720-866 Amadora, Portugal.